

# A scalar two-level boson model to study the IBM phase diagram in the Casten triangle

Julien Vidal,<sup>1</sup> José M. Arias,<sup>2</sup> Jorge Dukelsky,<sup>3</sup> and José Enrique García-Ramos<sup>4</sup>

<sup>1</sup>*Laboratoire de Physique Théorique de la Matière Condensée, CNRS UMR 7600, Université Pierre et Marie Curie, 4 Place Jussieu, 75252 Paris Cedex 05, France*

<sup>2</sup>*Departamento de Física Atómica, Molecular y Nuclear, Facultad de Física, Universidad de Sevilla, Apartado 1065, 41080 Sevilla, Spain*

<sup>3</sup>*Instituto de Estructura de la Materia, CSIC, Serrano 123, 28006 Madrid, Spain*

<sup>4</sup>*Departamento de Física Aplicada, Universidad de Huelva, 21071 Huelva, Spain*

We introduce a simple two-level boson model with the same energy surface as the Q-consistent Interacting Boson Model Hamiltonian. The model can be diagonalized for large number of bosons and the results used to check analytical finite-size corrections to the energy gap and the order parameter in the critical region.

PACS numbers: 21.60.Fw, 21.10.Re, 75.40.Cx, 73.43.Nq

## I. INTRODUCTION

The study of quantum phase transitions is a hot topic covering different branches of quantum many-body physics. In recent years, the study of low-dimensional lattice models has been triggered by the increasing interest on the development of a quantum computer. Moreover, concepts of quantum information have been used to characterize quantum critical phenomena. On a different respect, there is a revival of the study of structural changes in finite-size systems where precursors of the transitions could be observed [1]. In atomic nuclei, the Interacting Boson Model (IBM) [2] provides a framework simple but still detailed in which first and second order phase transitions can be studied. In fact, the transition from the spherical  $U(5)$  dynamical symmetry to the deformed  $\gamma$ -unstable  $O(6)$  dynamical symmetry has been extensively studied in the last few years [3, 4, 5]. The Hamiltonian describing this transition is a repulsive boson pairing Hamiltonian that has the particularity of being exactly solvable allowing the study of very large systems. The boson pairing model was first solved by Richardson [6] and more recently applied to the IBM [7, 8, 9]. However, this is the only integrable line in the phase diagram of the IBM often described with the Q-Consistent Hamiltonian (QCH) [10] and pictorially represented by the Casten triangle. This integrable line corresponds to one side of the triangle. Therefore, the interior area of the triangle as well as the other two sides are out of reach of large scale numerical studies. Numerical calculations in these cases are then limited by the number of bosons that standard IBM codes can manage, which are of the order of  $10^2$  bosons. However, strictly speaking quantum phase transitions only occur in macroscopic systems. Thus, it is of great interest to be able to extend previous analysis in the Casten triangle to a significant larger number of bosons.

In this paper, we introduce a simple two-level boson model depending on two control parameters, that leads to the same energy surface as the Q-consistent IBM Hamiltonian when the  $\gamma$  degree of freedom is frozen at  $\gamma = 0$ . In

other words, both energy surfaces coincide if axial symmetry is imposed in the IBM treatment. This model can be solved for very large boson numbers and it allows us to investigate the properties of the first-order phase transition from spherical to deformed axial shapes in the IBM. The two-level boson model can be viewed as a generalized Lipkin model with parity breaking terms, as a two coupled large spin system [11] or as a model to study tunnelling dynamics between two minima [12].

In Sect. II, after a brief presentation of the model, we derive its energy surface. Next, in Sect. III we compute the finite-size corrections up to order  $(1/N)^1$  in the spherical phase which allows us to discuss the finite-size behaviour at the critical point for different quantities such as the ground state energy, the gap, and the order parameter. Finally, Sect. IV is for summarizing.

## II. THE MODEL

Let us now introduce the two-level boson model whose Hamiltonian is

$$H = x n_t - \frac{1-x}{N} Q^y Q^y, \quad (1)$$

where the operators  $n_t$  and  $Q^y$  are defined as

$$n_t = t^\dagger t, \quad Q^y = s^\dagger t + t^\dagger s + y t^\dagger t \quad (2)$$

in terms of two species of scalar bosons  $s$  and  $t$ ,  $x$  and  $y$  being two independent control parameters. The total number of bosons  $N = n_s + n_t$  is a conserved quantity. The connection between the Hamiltonian (1) and a generalized Lipkin model or a two-spin model can be obtained by making the inverse of the Schwinger transformation  $K^+ = t^\dagger s$ ,  $K^- = s^\dagger t$ , and  $K^0 = \frac{1}{2}(t^\dagger t - s^\dagger s)$ .

We have deliberately written the two-level boson Hamiltonian in the form (1) to resemble QCH, where  $s$  and  $t$  play the role of the  $s$  and  $d_\mu$  bosons of the IBM respectively. Clearly, the difference resides on the quadrupolar character of the  $d_\mu$  boson leading to the

$U(6)$  algebra of the IBM, while our model is described by a  $U(2)$  algebra. Despite of this important difference, the  $st$  model captures the main characteristics of the phase diagram of IBM as we will now show.

The phase diagram of model (1) can be easily obtained in the coherent state approach. Therefore, we introduce a variational state of the form

$$|N, \beta\rangle = e^{\sqrt{\frac{N}{1+\beta^2}}(s^\dagger + \beta t^\dagger)} |0\rangle \quad (3)$$

where  $|0\rangle$  denotes the boson vacuum. The corresponding energy surface as a function of the variational parameter  $\beta$ , in the large  $N$  limit, is given by:

$$\begin{aligned} E(N, \beta) &= \langle N, \beta | H | N, \beta \rangle \\ &= N \frac{\beta^2}{(1 + \beta^2)^2} \left\{ 5x - 4 + 4\beta y(x - 1) + \right. \\ &\quad \left. \beta^2 [x + y^2(x - 1)] \right\}. \end{aligned} \quad (4)$$

Minimization of the energy (4) with respect to  $\beta$ , for given values of the control parameters  $x$  and  $y$ , gives the equilibrium value  $\beta_0$  defining the phase of the system.  $\beta_0 = 0$  corresponds to the symmetric phase, and  $\beta_0 \neq 0$  to the broken symmetry phase. Here, we restrict the study to the range  $x \in [0, 1]$  and  $y > 0$  which implies  $\beta_0 \geq 0$ . However, the treatment can be easily extended to the whole parameter space.

The schematic phase diagram of the  $st$  model is presented in Fig. 1 in the region of interest around the phase transition. In addition to the critical line displayed by the solid curve, we show the spinodal and antispinodal lines where the second minimum in the energy surface (4) starts to appear indicating a region in which both phases coexist.

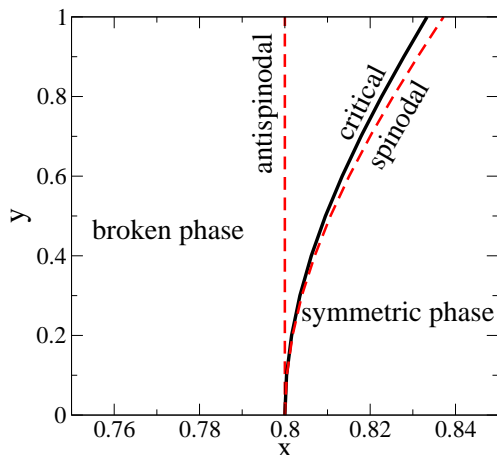


FIG. 1: (Color online) Phase diagram for the Hamiltonian (1) in the plane of the control parameters  $(x, y)$ . For  $y = 0$ , the transition is second-order whereas it is first-order otherwise.

For  $y = 0$ , there is an isolated point of second order phase transition as a function of  $x$ . Spinodal, antispinodal and critical point coincide at the critical value

$x_c = 4/5$ . For  $y \neq 0$  the phase transition changes its character to first order as can be seen in Fig. 2 for  $y = 1/\sqrt{2}$ . Schematically, for  $x = 1$ , the system is in the symmetric phase since the energy surface has a unique minimum at  $\beta = 0$ . When  $x$  decreases, one reaches the spinodal point ( $x = 0.82036$  for  $y = 1/\sqrt{2}$ ) where a second local (nonsymmetric) minimum ( $\beta \neq 0$ ) arises. This nonsymmetric minimum competes with the symmetric one till both attain the same depth at the critical point  $x_c = (4 + y^2)/(5 + y^2)$ . Beyond this value, the symmetric minimum at  $\beta = 0$  becomes a local minimum till  $x = 4/5$  where it becomes unstable (anti-spinodal point). We show in Fig. 2, (left panels), a sketch of this evolution for the special cases  $y = 0, 1/\sqrt{2}$ . The right panels in Fig. 2 show two cases in the coexistence region.

It is worth mentioning that this scheme is exactly the same as the one obtained in the IBM of nuclear structure. In fact the value  $y = 1/\sqrt{2}$  is equivalent to  $\chi = -\sqrt{7}/2$  describing the  $U(5)$  to  $SU(3)$  side of the Casten triangle [13] as we are showing now. The energy (4) coincides with that of the Q-consistent IBM-1 Hamiltonian in the thermodynamic limit (large  $N$ ). This correspondance is readily established if we write the Q-consistent IBM-1 Hamiltonian

$$H_{IBM} = x n_d - \frac{1-x}{N} Q^x \cdot Q^x, \quad (5)$$

where  $n_d$  is the  $d$ -boson number operator and  $Q^x$  is defined as

$$Q^x = s^\dagger \tilde{d} + d^\dagger s + \chi \left( d^\dagger \times \tilde{d} \right)^{(2)}, \quad (6)$$

with  $\chi$  the structure parameter of the quadrupole operator of the IBM. For the Hamiltonian (5) the energy surface in the large  $N$  limit reads (see for instance Eq. (6) in Ref. [21] taking the large  $N$  limit and  $\gamma = 0$ , this last condition is not a restriction since it is known that the IBM-1 including up to two-body interactions does not produce triaxiality)

$$\begin{aligned} E_{IBM}(N, \beta) &= \langle N, \beta | H_{IBM} | N, \beta \rangle \\ &= N \frac{\beta^2}{(1 + \beta^2)^2} \left\{ 5x - 4 - 4\sqrt{\frac{2}{7}}\beta\chi(x - 1) + \right. \\ &\quad \left. \beta^2 \left[ x + \frac{2}{7} \chi^2(x - 1) \right] \right\}. \end{aligned} \quad (7)$$

The equivalence between (4) and (7) is readily established in the thermodynamical limit setting  $y = -\sqrt{2/7}\chi$ . This correspondence can also be obtained from (6) if one is restricted to the spherical  $\mu = 0$  component of the  $d$ -bosons. In that case

$$Q = s^\dagger \tilde{d}_0 + d_0^\dagger s + \chi \langle 2020 | 20 \rangle d_0^\dagger \tilde{d}_0, \quad (8)$$

with the Clebsch-Gordan coefficient  $\langle 2020 | 20 \rangle = -\sqrt{2/7}$ . It should be clear that this equivalence is only valid in the thermodynamical limit and restricted to the scalar excitations. Differences between both models are due

to the fluctuations induced by the  $\gamma$ -vibration over the mean field. The present scalar model does not include  $K = 2$  excitations and consequently can not be used to study  $\gamma$ -excitations. But, apart from that, it mimics the usual representation of the IBM in a Casten triangle as shown in Fig. 3, where any point in the triangle can be described in polar coordinates  $(\rho, \theta)$ . The radial variable  $\rho$  is related to  $x$  (basically  $\rho = 1 - x$ ) and the angular variable  $\theta$  is related to  $y$  ( $\theta = (1 - \sqrt{2}y)\pi/3$ ) (or  $\chi$  in the IBM). Thus, changing the control parameters  $(x, y)$  (or  $x, \chi$  in IBM) one can reach any point in the triangle and, consequently analyze any trajectory in it looking for critical phenomena. In this respect, the present model allows to perform numerical calculations within the Casten triangle for large  $N$  values, which are not possible with the usual IBM codes and are needed to check finite-size corrections of different observables as we will show in the next section.

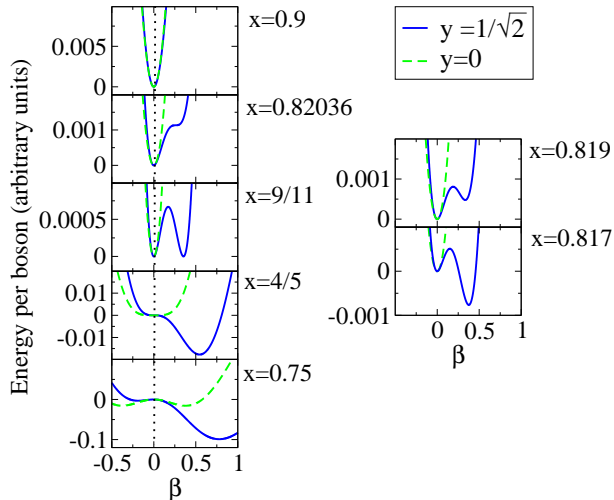


FIG. 2: (Color online) Energy surfaces for the Hamiltonian (1) in the large  $N$  limit (4) for  $y = 1/\sqrt{2}$  (full line) and  $y = 0$  (broken line) and for different  $x$ -values as a function of the deformation parameter  $\beta$ . The limits of the coexistence region are shown in the panels  $x = 0.82036\dots$  (spinodal) and  $x = 4/5$  (antispinodal). The critical point is represented in the middle (left) panel ( $x = 9/11$ ). The two panels on the right show two cases in the coexistence region.

We would like to emphasize here that the  $st$  boson model has a natural order parameter, the expectation value of the  $t$ -boson number operator  $n_t$ . This is not the case in the spin representation of the model [11]. On this regard, the Schwinger mapping could be used to translate the number operator  $n_t$  into spin operators suggesting an order parameter for the latter model. In the coherent state representation ( $N \rightarrow \infty$ ) the expectation value of the  $t$ -boson number operator is simply given by  $\langle n_t \rangle / N = \beta^2 / (1 + \beta^2)$ . For  $x = 1$ , this order parameter vanishes whereas for  $x = 0$  it is given by  $1 - \frac{2}{4 + y^2 + \sqrt{y^2(4 + y^2)}}$ . At the transition point  $x_c$ , both minima lead to the same energy and the jump of the order parameter is  $y^2 / (4 +$

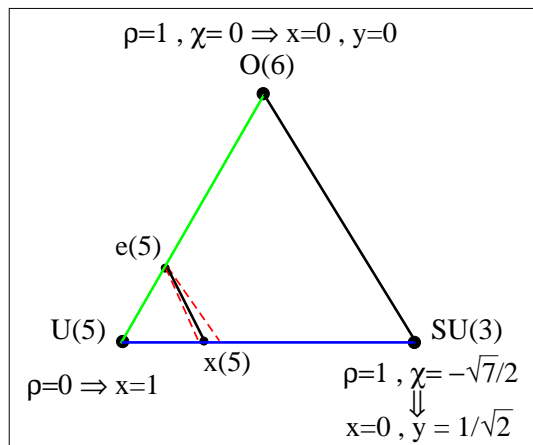


FIG. 3: (Color online) Usual representation of the IBM phase diagram as a Casten triangle. The three dynamical symmetries are located in the vertices. Critical points  $e(5)$  (second order) and  $x(5)$  (first order) with the coexistence region are also included. Variation of the control parameters, either in IBM or in the present model, allows to explore the whole model space represented by the triangle.

$y^2$ ) which vanishes, as expected, for  $y = 0$ . We have displayed in Fig. 4 the behaviour of the order parameter as a function of  $x$  for two different values of  $y$ .

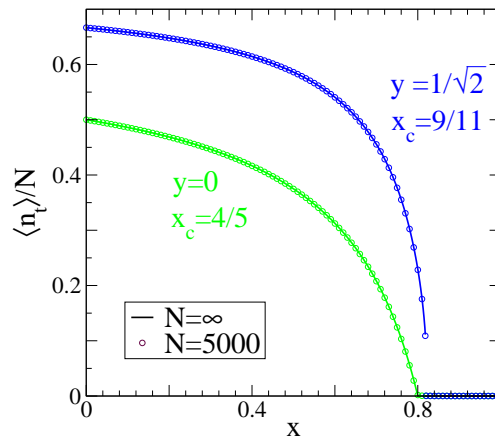


FIG. 4: (Color online) Variation of the order parameter as a function of  $x$  near the critical point. Full line are the analytical results for  $N = \infty$  and circles are numerical results for  $N = 5000$ . The jump is clearly observed for  $y \neq 0$ .

### III. FINITE SIZE CORRECTIONS: BEYOND MEAN FIELD

For  $y = 0$ , the  $st$  model corresponds, up to some re-definitions of the parameters, to the LMG model which has been recently shown to display nontrivial finite-size scaling properties at the transition point [14, 15, 16]. As explained above, the transition for  $y \neq 0$  is of first order and it is thus natural to expect some qualitative changes

for the finite-size corrections. To analyze them, we follow the same route as those detailed in Ref. [15] for  $y = 0$ .

For sake of clarity, we briefly sketch now this approach in the symmetric phase and refer to Ref. [17] for more details. For  $x > x_c$ , we map the one-body operators using the Holstein-Primakoff boson expansion [18] onto a single  $b$ -boson

$$t^\dagger t = b^\dagger b, \quad (9)$$

$$t^\dagger s = N^{1/2} b^\dagger (1 - n_b/N)^{1/2} = (s^\dagger t)^\dagger, \quad (10)$$

$$s^\dagger s = N - n_b. \quad (11)$$

with  $\langle n_b \rangle/N \ll 1$ . At order  $p$ , in the symmetric phase, the Hamiltonian schematically reads:

$$H = \sum_{i=0}^p \frac{H_i}{N^i} + O(1/N^{p+1}). \quad (12)$$

We make use of the canonical transformation method which allows to diagonalize exactly the Hamiltonian order by order. At order  $(1/N)^0$ ,  $H$  is simply a quadratic form and is thus simply diagonalized via a Bogoliubov

transform. As explained in Ref. [19], diagonalizing  $H$  beyond this order only requires to solve a linear set of algebraic equations. More concretely, let us introduce the  $a$ -boson through:

$$b^\dagger = \sum_{j=0}^p \frac{1}{N^j} \sum_{k,l} \alpha_{k,l}^{(j)} a^{\dagger k} a^{\dagger l}, \quad (13)$$

where the  $\alpha_{k,l}^{(j)}$  are coefficients to be determined such that  $H$  expanded at order  $1/N^p$  is a polynomial function in  $n_a$ . Further, one also has to impose the bosonic commutation rules which reads  $[b, b^\dagger] = 1$ . At each order, the content in  $a^\dagger$  and  $a$  is given by a simple power counting analysis. For  $p = 0$ , this transformation is nothing but the Bogoliubov transformation  $b^\dagger = \alpha_{1,0}^{(0)} a^\dagger + \alpha_{0,1}^{(0)} a$  and we thus have two coefficients to determine which are solutions of quadratic equations. At order  $p = 1$ , one must include linear and cubic terms and we have six coefficients  $\alpha_{k,l}^{(1)}$  to find which are now solutions of a linear set of equations. One then gets, at order  $1/N$ , the following diagonal form of the Hamiltonian:

---


$$\begin{aligned}
H = & \frac{1}{2} \left[ -x + \Xi(x)^{1/2} \right] + \\
& \frac{x^2(x-1)}{2N} \left[ \frac{-8 + 26x - 20x^2 + y^2(-2 + 6x - 3x^2)}{\Xi(x)^2} + x \frac{32 - 80x + 50x^2 + y^2(8 - 14x + 5x^2)}{\Xi(x)^{5/2}} \right] + \\
& n_a \left\{ \Xi(x)^{1/2} + \frac{x^2(x-1)}{N} \left[ \frac{-8 + 10x + y^2(-2 + x)}{\Xi(x)^{3/2}} + \frac{-16 + 52x - 40x^2 + y^2(-4 + 16x - 10x^2)}{\Xi(x)^2} \right] \right\} + \\
& : n_a^2 : \frac{x^2(x-1)}{N} \frac{-8 + 26x - 20x^2 + y^2(-2 + 8x - 5x^2)}{\Xi(x)^2} + O(1/N^2), \quad (14)
\end{aligned}$$


---

with  $\Xi(x) = x(5x - 4)$ . As can be readily seen, the ground state energy as well as the gap are regular functions provided  $x > 4/5$  which is the value of the critical point for  $y = 0$ . For nonvanishing  $y$ , it means that for  $x \geq x_c > 4/5$ , there is no divergence in these quantities. One thus naively expect some  $1/N$  corrections from this side of the transition.

The same approach can obviously be applied in the broken phase to diagonalize  $H$  at the same order. It then requires the exact knowledge of  $\beta_0$  which is solution of the cubic equation  $\partial E(N, \beta)/\partial \beta = 0$ . If, for arbitrary  $0 < x < x_c$ , it is a complicated expression of  $x$  and  $y$ , the nonvanishing solution for  $x = x_c$  simply reads  $\beta_0 = y/2$  and thus allows for simplifications. The main result of this study is that the Hamiltonian expanded at order  $1/N$  is exactly the same at the critical point  $x = x_c$  for  $\beta_0 = 0$  and  $\beta_0 = y/2$ . Of course, at order  $N$ , one finds  $H = 0$  which simply confirms the existence

of a first order quantum phase transition. The most interesting point is that the finite-size corrections are also the same for both values of  $\beta_0$ . Physically, it means that for  $x = x_c^\pm$  the gap is  $\Delta = \Xi(x_c)^{1/2} + O(1/N)$  but for  $x = x_c$ , the gap must vanish in the large  $N$  limit. In Fig. 5 we show the behaviour of the gap in the region around the critical point,  $x_c = 9/11$ , for  $y = 1/\sqrt{2}$ . As can be seen gaps in the symmetric and the broken phases are indeed equal at  $x = x_c^\pm$ . However, exactly at the critical point both states are degenerated giving rise to a zero gap as indicated by the black dot at  $x_c = 9/11$ . In the inset, we show the behaviour of the gap at the critical point as a function of the boson number  $N$ , confirming the predicted exponential  $\Delta \sim e^{-AN}$ . The exponent  $A$  is a function of  $y$  that vanishes in the limit  $y = 0$  where we expect  $\Delta \sim N^{-1/3}$  [20]. This exponential decay clearly indicates that the  $1/N$  expansions from the symmetric phase ( $\beta_0 = 0$ ) and from the broken one ( $\beta_0 = y/2$ ) are

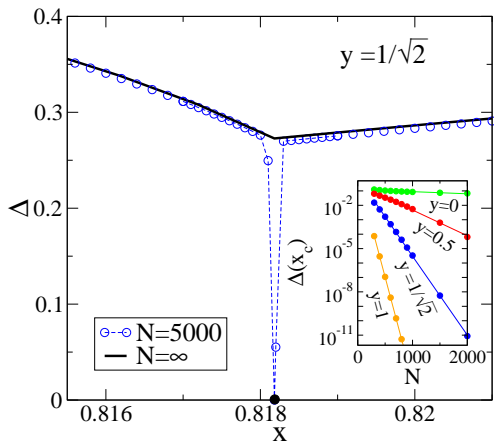


FIG. 5: (Color online) Behaviour of the gap as a function of  $x$  near the critical point for  $y = 1/\sqrt{2}$ . The full bold line and the full dot at  $x_c = 9/11$  correspond to the analytical results. Open dots are the numerical calculation for  $N = 5000$ . In the inset, the exponential decrease of the gap at the critical point is shown for several values of  $y$ .

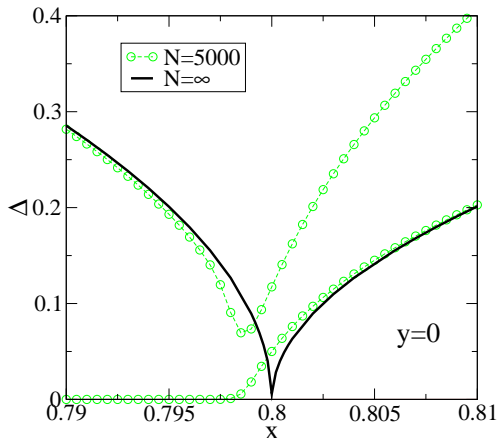


FIG. 6: (Color online) Same as Fig. 5 but for  $y = 0$ . The full line is the analytical result for the gap, while the open dots correspond to the first two excited states for  $N = 5000$ .

the same at all orders since any difference would imply a power-law decrease. As will be discussed in a forthcoming publication for the standard IBM model, we emphasize that this matching of the  $1/N$  expansions is not a rule but rather an exception [17]. In Fig. 6 the gap for  $y = 0$  is shown in the region around the critical point. The full line corresponds to the analytical expression and vanishes at the critical point. In this case, there are no parity breaking terms so results discussed in Ref. [15]

are recovered. For  $x > 4/5$ , the system is in the symmetric phase with positive parity. The gap is related to the energy of the first excited state corresponding to a one phonon state with negative parity. The second excited state is a two phonon state with positive parity. The excitation energies for these two states for  $N = 5000$  are plotted in Fig. 6 as circles joined by a (green) line. For  $x < 4/5$  the system is in the broken phase. In the limit  $x = 0$  there are two sets of states of different “parity” degenerated ( $\pm$  parity doublets) as displayed by the lowest (green) circle-line in Fig. 6. In this phase the nonvanishing gap is related to the excitation energy of a different phonon which corresponds to the upper (green) circle-line. It is equivalent to the  $\beta$  excitation in IBM (there are no  $\gamma$  excitation in this scalar model). In the limit  $N \rightarrow \infty$  both gaps (from the spherical and from the broken sides) go to zero at the critical point, although they remain finite at finite  $N$  as clearly seen in Fig. 6.

#### IV. SUMMARY AND CONCLUSIONS

To summarize, we have introduced a two-level model in terms of two scalar bosons  $s$  and  $t$ , whose phase diagram in the thermodynamical limit is the same as the IBM phase diagram when described by the QCH. We have exactly diagonalized the Hamiltonian in the symmetric phase up to order  $(1/N)^1$  and obtained the finite-size corrections for the ground state energy, the gap and the order parameter. These corrections were tested against numerical results for large systems. Though the phase diagram of this  $st$  model and the QCH coincide in the large  $N$  limit, beyond the mean-field level the QCH may have different properties due to the dynamics of fluctuations and correlations in the full  $(\beta, \gamma)$  space [21, 22, 23]. In particular, while our  $st$  model is fully integrable [24] the IBM is chaotic for  $\chi \neq 0$  [25] with the exception of the  $SU(3)$  symmetry limit. Extension of the formalism presented in this paper to the IBM will be the subject of a forthcoming publication [17].

#### V. ACKNOWLEDGMENTS

This work has been partially supported by the Spanish Ministerio de Educación y Ciencia and by the European regional development fund (FEDER) under projects number BFM2003-05316-C02-02, FIS2005-01105 and FPA2003-05958.

- [1] F. Iachello and N. V. Zamfir, Phys. Rev. Lett. **92**, 212501 (2004).  
 [2] F. Iachello and A. Arima, *The Interacting Boson Model* (Cambridge University Press, Cambridge, 1987).

- [3] J. Jolie, P. Cejnar, R. F. Casten, S. Heinze, A. Linnemann, and V. Werner, Phys. Rev. Lett. **89**, 182502 (2002).  
 [4] J. M. Arias, J. Dukelsky, and J. E. García-Ramos, Phys.

- Rev. Lett. **91**, 162502 (2003).
- [5] P. S. Turner and D. J. Rowe, Nucl. Phys. A **756**, 333 (2005).
- [6] R. W. Richardson, J. Math. Phys. **9**, 1327 (1968).
- [7] F. Pan and J. P. Draayer, Nucl. Phys. A **636**, 156 (1998).
- [8] J. Dukelsky and S. Pittel, Phys. Rev. Lett. **86**, 4791 (2001).
- [9] J. M. Arias, C. E. Alonso, A. Vitturi, J. E. García-Ramos, J. Dukelsky, and A. Frank, Phys. Rev. C **68**, 041302 (2003).
- [10] D. D. Warner and R. F. Casten, Phys. Rev. Lett. **48**, 1385 (1982).
- [11] D. A. Garanin and E. M. Chudnovsky, Phys. Rev. B **63**, 024418 (2000).
- [12] V. I. Belinicher, C. Providencia, and J. da Providencia, J. Phys. A **30**, 5633 (1997).
- [13] R. F. Casten and N. V. Zamfir, Phys. Rev. Lett. **85**, 3584 (2000).
- [14] S. Dusuel and J. Vidal, Phys. Rev. Lett. **93**, 237204 (2004).
- [15] S. Dusuel and J. Vidal, Phys. Rev. B **71**, 224420 (2005).
- [16] F. Leyvraz and W. D. Heiss, Phys. Rev. Lett. **95**, 050402 (2005).
- [17] J. Vidal, J. M. Arias, J. Dukelsky, and J. E. García-Ramos, in preparation.
- [18] T. Holstein and H. Primakoff, Phys. Rev. **58**, 1098 (1940).
- [19] J. Vidal and S. Dusuel, cond-mat/0510281.
- [20] S. Dusuel, J. Vidal, J. M. Arias, J. Dukelsky, and J. E. García-Ramos, Phys. Rev. C **72**, 011301(R) (2005).
- [21] P. Cejnar and J. Jolie, Phys. Rev. E **61**, 6237 (2000).
- [22] D. J. Rowe, P. S. Turner, and G. Rosensteel, Phys. Rev. Lett. **93**, 232502 (2004).
- [23] D. J. Rowe, Nucl. Phys. A **745**, 47 (2004).
- [24] L. Benet, C. Jung, and F. Leyvraz, J. Phys. A **36**, L217 (2003).
- [25] Y. Alhassid, A. Novoselsky, and N. Whelan, Phys. Rev. Lett. **65**, 2971 (1990).